Untangling the adolescent internalizing brain: investigations on brain networks in youth with anxious and depressive problems

Roelofs, E.F.

3

Longitudinal development of resting-state functional connectivity in adolescents with and without internalizing disorders

Eline F. Roelofs, Janna Marie Bas-Hoogendam, Anderson M. Winkler,
Nic J.A. van der Wee, Robert R. J. M. Vermeiren

Neurosci Appl 2024 Vol. 3

Abstract

Objective: Longitudinal studies using resting-state functional magnetic resonance imaging (rs-fMRI) focused on adolescent internalizing psychopathology are scarce and have mostly investigated standardized treatment effects on functional connectivity (FC) of the full amygdala. The role of amygdala subregions and large resting-state networks had yet to be elucidated, and treatment is in practice often personalized. Here, longitudinal FC development of amygdala subregions and whole-brain networks are investigated in a clinically representative sample.

Methods: Treatment-naïve adolescents with clinical depression and comorbid anxiety who started care-as-usual (n = 23; INT) and healthy controls (n = 24; HC) participated in rs-fMRI scans and questionnaires at baseline (before treatment) and after three months. Changes between and within groups over time in FC of the laterobasal amygdala (LBA), centromedial amygdala (CMA) and whole-brain networks derived from independent component analysis (ICA) were investigated.

Results: Groups differed significantly in FC development of the right LBA to the postcentral gyrus and the left LBA to the frontal pole. Within INT, FC to the frontal pole and postcentral gyrus changed over time while changes in FC of the right LBA were also linked to symptom change. No significant interactions were observed when considering FC from CMA bilateral seeds or within ICA-derived networks.

Conclusion: Results in this cohort suggest divergent longitudinal development of FC from bilateral LBA subregions in adolescents with internalizing disorders compared to healthy peers, possibly reflecting nonspecific treatment effects. Moreover, associations were found with symptom change. These results highlight the importance of differentiation of amygdala subregions in neuroimaging research in adolescents.

Introduction

Internalizing disorders like anxiety and depression often start in adolescence and are highly prevalent in this stage of life. Sadly, recent studies imply that comorbid anxiety disorders are rather the rule than the exception in clinically depressed adolescents, as more than 50% of adolescents with a clinical depression have one or more comorbid anxiety disorders [1]. These adolescents often display more severe symptoms, poorer response to treatment and increased risk of suicidal behaviors compared to clinically depressed adolescents without comorbid psychopathology [1]. Models suggest that complex interactions between environment, genes, neurobiological characteristics, and the timing of developmental stages contribute to the development of these mental illnesses [2-4]. To attain insights in neurobiological underpinnings of adolescent internalizing disorders, investigation of function and structure of neural networks is vital.

Activity of neural networks at rest, also called functional connectivity (FC), is widely investigated by use of resting-state functional MRI (rs-fMRI) [5, 6]. Rs-fMRI focuses on spontaneous, low-frequency fluctuations (<0.1 Hz) in the blood oxygenation level-dependent (BOLD) signal that occur in the absence of a task or stimulus, which can be used to identify functional neural networks [7-9]. Two common methods to identify these networks are seed-based correlation analysis (SCA), a hypothesis-driven approach to investigate the primary signal of a region-of-interest (ROI) to the whole brain [7], and independent component analysis (ICA), a fully data-driven, exploratory approach to extract resting-state networks using a multivariate exploratory analysis, which divides the brain into independent spatial regions according to their signal fluctuations [10]. To our knowledge, fully data driven approaches are still scarce in current literature despite their advantages, like being unbiased to a priori selected regions. When comparing SCA and ICA, secondary signals expressed by the brain are missed in SCA [7], whereas distinct signals occurring in a particular region can go unnoticed due to the limited number of components that is being extracted in ICA [10]. Therefore, SCA and ICA can be seen as complementary methods to investigate FC of neural networks and brain regions, such as the amygdala.

As one of the most extensively investigated brain regions in humans and animals, the function and structure of the amygdala is quite well known [11, 12]. It consists of several subregions, like the laterobasal amygdala (LBA), involved in regulation of fear and the perception hereof, and centromedial amygdala (CMA), mainly concerned with acute stress-reactions [11-13]. Recently, it has been hypothesized that these subregions each contribute to different aspects of mental disorders [12, 14], but their role in adolescent internalizing disorders has yet to be elucidated. Involvement of either or both subregions is likely, as meta-analyses of cross-sectional studies reported changes of full amygdala FC in depressed and anxious adolescents and adults when compared to healthy peers [15, 16], such as hypoconnectivity between the amygdala and the medial PFC [16], and decreased amygdala FC within the executive control network, which has been found in regulating emotions and initiating goal-directed responses [17] although a recent meta-analysis did not replicate these findings in depressed adolescents [18]. These alterations may underly the characteristic imbalance between affective-cognitive networks in adolescent internalizing disorders [19-21]. To expand the understanding of the course of these alterations, development of amygdala FC and its subregions needs to be investigated. Unfortunately,

longitudinal studies in this population are scarce and have reported inconsistent and isolated findings on full amygdala FC [2, 22-27], like increased FC of the amygdala to the right medial and middle frontal gyrus and decreased FC of the amygdala and the right posterior cingulate cortex, which were associated with decreases in depressive symptoms [23, 27]. These studies suggest a normalizing or compensatory effect of treatment on amygdala FC [2, 22-27], although this must be interpreted cautiously due to the scarcity of studies and their inconsistent, isolated results. Altogether, even though longitudinal studies are inconclusive, alterations in FC of amygdala subregions are highly suspect to be involved in adolescent internalizing disorders.

Current models suggest that several whole-brain resting-state networks are involved in internalizing disorders as well (for a comprehensive overview, see Table S2 and Figure 1 in [28]). Cross-sectional alterations in FC within and between these networks have been reported in depressed adolescents and anxious adults when compared to healthy peers, such inter- and intranetwork alterations in the limbic, default mode, central executive, and salience networks [15, 18, 29]. It is therefore likely that, in addition to the changes in amygdala FC, complex and widely spread changes in FC of other networks are involved in the development and course of adolescent internalizing disorders.

Besides the need to explore the longitudinal trajectory of FC of these regions and networks in this population, outcomes of prior longitudinal studies on FC development in adolescents with internalizing disorders may not reflect practical applicability in clinical settings, as they predominantly investigated treatment effects using standardized protocols [23-27]. In clinical practice, however, especially adolescents typically receive more personalized treatments tailored to their individual needs, adjusted to their level of emotional and cognitive development and in collaboration with their family [30-32].

To gain more insight in the development of neural networks, we have conducted the *Emotional Pathways' Imaging Study in Clinical Adolescents* (EPISCA) study [33]. In EPISCA, we used a study design in which participants received care-as-usual and were followed over the course of six months without study interventions, thus reflecting real world development of neural networks in a clinically heterogeneous group as close as possible. Using this longitudinal dataset, we have previously demonstrated that baseline measures of white matter microstructure are associated with changes in depressive symptoms over time in adolescents with internalizing disorders [34].

In the present study, FC in adolescents with internalizing disorders and healthy controls over a period of three months was investigated to obtain more insight in the development of FC of amygdala subregions and whole brain networks between and within these groups, possibly reflecting treatment effects. Based on previous findings, we expected FC differences between groups over time in regions involved in emotion processing, such as limbic structures, and emotion regulation, like frontal regions.

Methods

Participants

Data for this study were derived from the EPISCA study [33]. Briefly, two groups were investigated over time and in both groups, the majority of participants identified themselves as being female. The first group consisted of treatment-naïve adolescents with clinical depression and comorbid anxiety (internalizing disorders group, 'INT', n = 30 at baseline). They were included in the study before start of care-as-usual and were diagnosed with clinical depression and at least one clinical anxiety disorder as assessed by categorical measures of DSM-IV depressive or anxiety disorders. The second group consisted of healthy control peers (HC, n = 32 at baseline). All participants were investigated three times in a six-month timespan, during which the INT group received personalized variants of cognitive behavioral therapy (CBT) and family-based interventions. Extensive information about recruitment of participants, in- and exclusion criteria and demographic data of the full sample can be found in previous publications [33-56] and in the supplemental information. Detailed information about personalized treatments, MRI data acquisition, preprocessing of the rs-fMRI data and statistical analyses of demographical data, including multiple comparison corrections, is also included in supplemental information.

In the present study, rs-fMRI data obtained at baseline (before treatment; T1) and after three months (T2) were analyzed, as loss-to-follow-up was substantial after six months (loss-to-follow-up after three months: 16%, loss-to-follow-up after six months: 24%). At baseline, two participants (n = 1 INT, n = 1 HC) were excluded due to an anomaly on the structural T1-scan. Furthermore, one HC participant was excluded as criteria for clinical psychopathology were met. Two HC participants were excluded due to technical issues and six participants (n = 4 INT, n = 2 HC) did not follow-up after the first visit, leaving data from 25 INT and 26 HC participants for initial analysis. In addition, data from several questionnaires was included if available on both timepoints. To assess severity of depressive and anxious symptoms, total scores on the Children's Depression Inventory (CDI) [57] and on the anxiety subscale of the Revised Child Anxiety and Depression Scale (RCADS) [58] were included. Pubertal stage was taken into account by using baseline scores on the self-report Pubertal Development Scale (PDS) [59], according to the following categories: 1) prepubertal, 2) early pubertal, 3) midpubertal, 4) late pubertal, and 5) postpubertal.

General preprocessing of resting-state data

Image pre-processing and analyses were performed using the Oxford Centre for Functional Magnetic Resonance Imaging of the Brain (FMRIB) Software Library (FSL), version 6.0.3 (RRID:SCR_002823). Data underwent several preprocessing steps following the procedures described in [60-62]. First, non-brain removal was performed on T1 and high-resolution EPI data using the Brain Extraction Tool (BET) [63]. Then, BOLD data were preprocessed using FEAT (FMRI Expert Analysis Tool) [64], including motion correction using MCFLIRT [65], spatial smoothing using a Gaussian kernel of full-width half- maximum (FWHM) 6.0 mm and grand-mean intensity normalization of the entire 4D dataset by a single scaling factor to enable higher-level analyses and registration. Resting- state fMRI scans were

first registered to high-resolution EPI images, which were registered to T1 images, which in turn were registered to the Montreal Neurological Institute (MNI) T1-template brain (resolution 2 mm) using FNIRT nonlinear registration [65-67]. These transformation matrices were then combined to obtain a native-to-MNI-space transformation matrix per participant.

Next, ICA-AROMA (ICA-based Automatic Removal Of Motion Artifacts) was used to remove motion-related artefacts [60, 61]. Afterwards, native T1-weighted images were segmented into white matter (WM), central spinal fluid (CSF) and grey matter (GM) probability maps using FSL FAST [68]. Without extensive erosion of WM and CSF masks, these signals can be correlated with the GM signal [69]. Therefore, we applied 2 erosion cycles for the CSF mask and 4 erosion cycles for the WM mask to prevent partial voluming. If a mask contained fewer than 5 voxels after a given erosion cycle, the previous cycle was selected. Then, these masks were linearly aligned into native resting state space using FSL's FLIRT [65-67]. BOLD data were then submitted to FEAT to perform high-pass temporal filtering (Gaussian-weighted least-squares straight line fitting, cutoff 0.01 Hz) and subsequently nuisance regression with WM and CSF masks was performed. The processed resting-state fMRI data of each participant were then warped to MNI space using the combined native-to-MNI transformation matrix.

Data quality was assessed by inspecting each participant's processed EPI data as a time series (i.e., "carpet plot") alongside framewise displacement (FD), as calculated by FSL_motion_outliers. Participants were excluded if mean FD over time was > 0.2 mm, or > 20% suprathreshold FDs, or any FD > 5.0 mm [62].

Identification of resting-state networks

Rs-fMRI data were investigated twofold using the Oxford Centre for Functional Magnetic Resonance Imaging of the Brain (FMRIB) Software Library, version 6.0.3 (FSL; RRID:SCR_002823). First, SCA was used to investigate FC of two bilateral amygdala subregions, creating seeds derived from the Juelich histological atlas [44]. In short, voxelwise bilateral regions-of-interest (ROIs) of the laterobasal amygdala (LBA) and centromedial amygdala (CMA) were created by including voxels only if the probability of the voxel belonging to either subregion was higher than 40%. Each voxel was exclusively assigned to one region, overlapping voxels were assigned to the region with the greatest probability. Using these ROIs as seeds, FC of each subregion to the whole brain was investigated. First, we explored FC of each subregion for every individual participant on each timepoint. These results, containing data from both timepoints and all participants, were subsequently used as input to generate group-level FC maps of each subregion to the whole brain, using a cluster-forming threshold of $Z > 3.1$ and a cluster-corrected extent threshold $p < 0.05$ (Figure 1B and Table S2). The activated networks were successively binarized and used as a mask for the statistical analyses below, ensuring that analyses were confined within the respective networks.

Second, to determine group-level data-driven resting-state networks, Probabilistic Independent Component Analysis (PICA) [70] and dual regression analysis [71] were used. First, PICA was applied to separate 4D functional data into spatial maps with an associated time course for each map, starting with temporally concatenating all preprocessed subjects' data for both timepoints in Montreal Neurological

Institute (MNI)-standard space into one dataset. Subsequently, this dataset was decomposed in 20 independent components, consisting of independent vectors describing signal variation across the spatial (maps) and temporal (time-course) domain. This number of components results in a representative set of functional connectivity networks [72] in line with previous work in our group [73]. Afterwards, dual regression was used to generate subject-level maps for each of the 20 group components. This resulted in a set of maps (one for each original group-level ICA component) that describe the network structure based on the data from each participant. The 20 spatial maps at group-level were visually inspected. Components with spatial similarity to the networks of interest were selected based on descriptions of functional networks in previous work: default mode, dorsal attention, frontoparietal (separated in a left and right component), executive control, salience and affective network (Figure 1A and Table S2) [72, 74-76].

Statistical analysis of resting-state networks

After investigating FC of the LBA and CMA seeds (Figure 1B) and confirming the seven networks as defined by ICA (Figure 1A), further statistical analyses were conducted. First, differences in head motion between groups were investigated by comparing individual mean relative and absolute motion parameters created by FSL's MCFLIRT using the Mann-Whitney U test in R (Table 1; R Project for Statistical Computing (RRID:SCR_001905)) [65, 77].

Then, several analyses were conducted. First, SCA was applied to explore group x time interactions in connectivity of two bilateral amygdala subregions, namely the LBA and CMA. To underline the importance of investigating subregions, we conducted additional analyses using bilateral whole amygdala seeds. Second, exploratory group x time interactions were investigated in seven resting-state networks derived from ICA: default mode, frontoparietal (separated in a left and right component), executive control, dorsal attention, salience and affective network [72-76, 78]. Specifically, multi-level block permutation analyses were conducted in FSL's PALM [79, 80] (RRID:SCR_017029) to examine voxel-wise changes in FC in the networks of interest (four networks related to bilateral amygdala subregions; seven whole-brain networks) over time between INT and HC, using 5000 permutations and threshold-free cluster enhancement (TFCE) [81]. Two contrasts were investigated in each time direction: i) group x time interaction HC (T2 > T1) > INT (T2 > T1) and ii) group x time interaction INT (T2 > T1) > HC (T2 > T1). In other words, the first interaction explores for each voxel within the functional networks whether HC had a greater change in FC after three months than INT, while the second interaction investigates whether the change in FC after three months was greater in INT compared to HC (design is provided in Table S3). Age at the time of scanning was accounted for by subject-specific regressors. To assure these assumptions, additional analyses were conducted to control the effect of age on group x time interactions by adding age at baseline as a fixed, non-time varying covariate. Two extra contrasts were added to the main design to test positive and negative effects of age on changes in FC. Results are compared to the main design in the Supplemental Text (Table S7 and Figure S1). Correction for multiple testing considered the fact that we investigated both directions for interaction effects [82]. Analyses across seeds and hemispheres were corrected for multiple comparisons at a false discovery

rate (FDR) of 5% [83]. In case of a significant interaction, directionality of the interaction within each group was explored (Table S3) and a separate design was used to investigate whether changes in FC were associated with symptom change within INT (Table S4). Multi-level block permutation analyses were conducted in PALM with 5000 permutations and TFCE to investigate associations with changes in anxiety symptoms, as measured by the RCADS, and changes in depressive symptoms, as measured by the CDI. An F-test was added to assess their overall effects on FC change, which reflects significance without providing directionality or a joint score of both symptom scores. INT-participants were included in these association analyses if the questionnaire (RCADS and/or CDI) was filled out on baseline (before treatment) and after three months.

Results

Exclusion of participants

After motion control, four participants ($n = 2$ INT, $n = 2$ HC) were excluded, leaving 23 INT participants and 24 HC participants for further analysis. Motion parameters were not significantly different between INT and HC (Table 1).

Table 1 Motion parameters.

	INT (n = 23)	HC (n = 24)
Head motion (median ± SD)		
mean absolute head motion T1	0.18 ± 0.10	0.16 ± 0.08
mean relative head motion T1	0.07 ± 0.02	0.08 ± 0.02
mean absolute head motion T2	0.22 ± 0.12	0.17 ± 0.19
mean relative head motion T2	0.08 ± 0.02	0.08 ± 0.02

Demographics

Characteristics of the final sample are summarized in Table 2. Groups did not differ in demographic measurements. As expected, patients experienced significantly higher levels of depression and anxiety on both timepoints compared to healthy controls ($p < 0.000$). Within INT, depression and anxiety severity significantly decreased over time ($p = 0.017$, $p < 0.001$, resp.). There were no significant symptom changes within HC.

Table 2 Demographic characteristics of participants with and without clinical depression and comorbid anxiety.

	INT (n = 23)	HC (n = 24)
Demographics at baseline		
Age in years (mean ± SD; range)	15.86 ± 1.47 (13 - 18)	15.12 ± 1.74 (12 - 20)
Male / Female (n)	2 / 21	3 / 21
IQ (mean ± SD)	105.30 ± 8.35	107.08 ± 7.92
Puberty stage (median ± SD; range) [a]	4.00 ± 0.73 (2 – 5)	4.00 ± 0.73 (3 – 5)
Days between visits (median ± SD)	100.00 ± 11.76	98.00 ± 12.59
Ethnicity (% white)	91.30	95.83
Primary diagnoses [b] (n)		
MDD + GAD	15	
MDD + SAD	13	
MDD + specific phobia	8	
MDD + panic disorder	4	
MDD + separation anxiety	7	
Secondary (externalizing) diagnoses [b] (n)		
ADHD; inattention	1	
ADHD; hyperactive	1	
Oppositional Defiant Disorder	1	
Behavioral Disorder	1	
Self-report measures (median ± SD)		
CDI on baseline [c]	20.00 ± 9.20	4.00 ± 3.62
CDI after three months	11.50 ± 9.40	2.00 ± 3.31
RCADS on baseline	33.0 ± 14.70	10.00 ± 11.14
RCADS after three months [d]	25.00 ± 15.56	10.00 ± 8.60

MDD: Major Depressive Disorder; GAD: Generalized Anxiety Disorder; SAD: Social Anxiety Disorder; ADHD: Attention Deficit Hyperactivity Disorder; CDI: Children's Depression Inventory; RCADS: Revised Child Anxiety and Depression Scale; SD: Standard Deviation. [a] Diagnoses are not mutually exclusive. [b] Three healthy controls and two patients did not complete the questionnaire. [c] One patient did not complete the questionnaire. [d] Two patients did not complete the questionnaire.

Voxelwise changes in FC over time between patients and controls

Significant group x time interactions were found in FC of the left and right LBA (Table 3; Figure 1C/1D). Specifically, development of FC between the left LBA and frontal pole (Figure 1C; Table 3) was significantly different between INT and HC. Furthermore, significant differences were found in development of FC between the right LBA and right postcentral gyrus between INT and HC (Figure 1D; Table 3). However, results did not stand when corrections for multiple testing were applied. No

significant interactions were observed within the ICA-defined networks or in FC of the CMA or whole amygdala bilateral seeds.

Voxelwise changes in FC over time within patients and controls

Additional analyses concerning the left and right LBA further revealed effects of time within INT (Table S6). Figure 1E/1F illustrates the change in z-score between and within the groups, indicating an increase of FC in the INT group and a decrease in the HC group of the bilateral LBA seeds over time. Results were not significant at the FDR-corrected level. At the uncorrected level, FC of the left LBA significantly increased to the frontal pole (Figure 1E) and decreased to the postcentral gyrus, but FC of the right LBA did not significantly change. FC did not significantly change over time within HC.

Associations with symptom changes in significant clusters

Within INT, associations between changes in symptom scores and changes in FC of each LBA seed were further explored. There were no significant associations at the corrected significance level, but an association was found between changes of FC between the right LBA and the postcentral gyrus and the overall effect of changes in anxious and depressive symptoms at the uncorrected level (Table S6) ($p = 0.032$, 30 voxels; $p = 0.037$, 13 voxels; $p = 0.049$, 3 voxels. TFCE and FWE corrected at p-values < 0.05). Figure 2 illustrates the associations between changes in symptoms and changes in FC of the right LBA, indicating an association between a decrease of symptoms and an increase of FC of right LBA to the postcentral gyrus. This association was only significant when analyzing the joint effect of anxious and depressed symptoms. Correlation analyses between changes in FC of LBA seeds and changes in anxious or depressive symptoms separately did not reveal any significant associations.

Table 3 Coordinates of significant clusters in group x time interaction.

	Voxels	p-value	MNI coordinates			Regions involved
			X	Y	Z	
Left LBA seed	581	0.003	0	50	-6	Frontal Pole; Frontal Medial Cortex; Paracingulate Gyrus; Anterior Cingulate Gyrus
Right LBA seed	74	0.021	60	-12	18	Postcentral Gyrus; Central Opercular Cortex

LBA: laterobasal amygdala. Threshold-free cluster enhancement (TFCE) and family-wise error (FWE) corrected at p-values < 0.05.

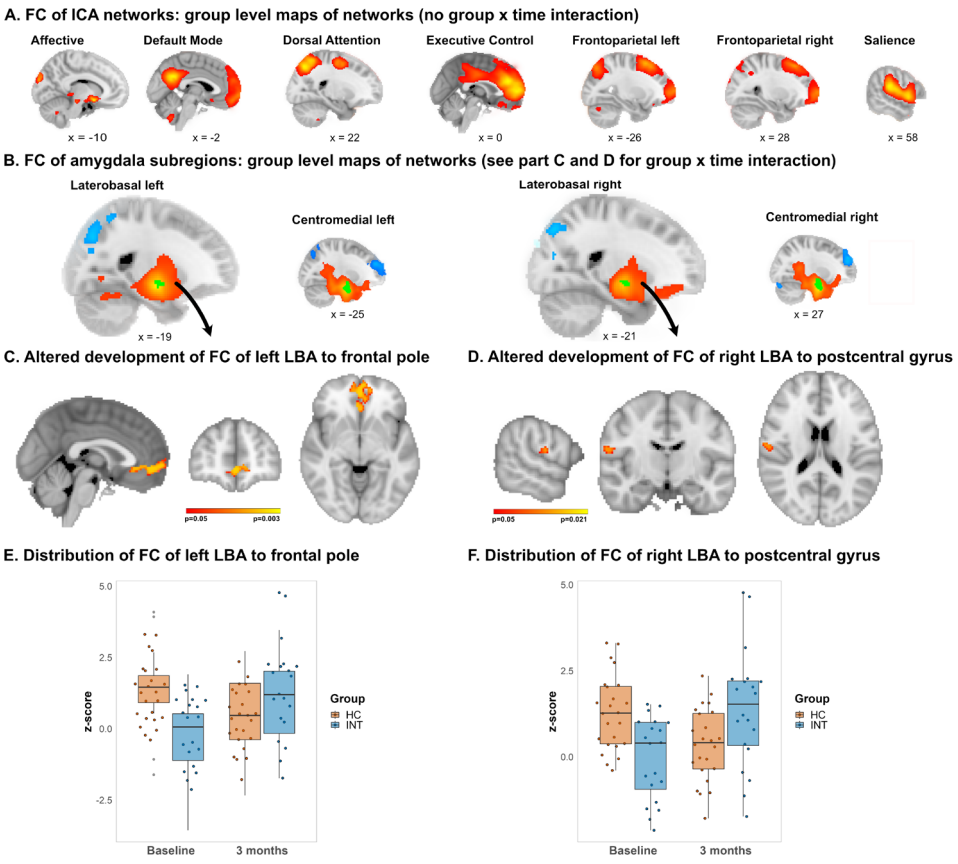

Figure 1 Different development of LBA FC in adolescents with internalizing disorders compared to healthy peers. (a) FC of networks derived from data-driven ICA analysis. (b) Positive (red) and negative (blue) FC of networks derived from SCA using amygdala subregions as seeds (green). (c) Significant group x time interaction in left LBA FC to the frontal pole (INT (T2 > T1) > HC (T2 > T1)), coordinates of displayed slices (MNI, x, y, z): 0, 50, -6. (d) Significant group x time interaction in right LBA FC to the postcentral gyrus (INT (T2 > T1) > HC (T2 > T1)), coordinates of displayed slices (MNI, x, y, z): 60, -12, 18. (e) Distribution of mean z-scores for INT and HC on baseline and after three months in the significant cluster in the frontal pole. Dots represent individual z-scores. (f) Distribution of mean z-scores for INT and HC on baseline and after three months in the significant cluster in the postcentral gyrus. Dots represent individual z-scores. Images are displayed according to radiological convention: right in image is left in the brain. LBA: laterobasal amygdala; INT: internalizing group; HC: healthy controls; MNI: Montreal Neurological Institute.

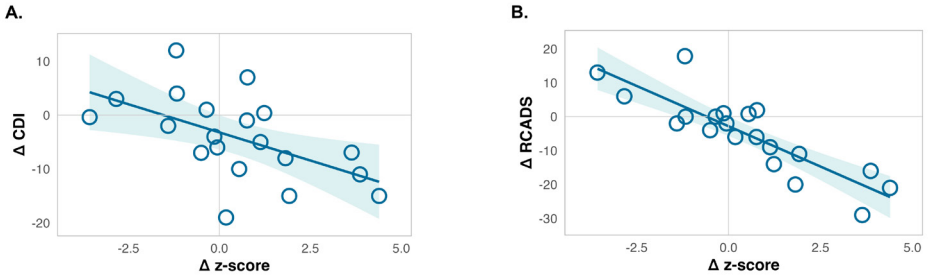

Figure 2 Associations between longitudinal changes in anxious and depressive symptoms and changes in functional connectivity between the right LBA and the postcentral gyrus within adolescents with depression and comorbid anxiety. (a) Association between changes in depressive symptoms (D CDI) and changes in functional connectivity (D z-score). Changes are calculated as score after three months minus score on baseline. Dots represent individual associations between changes in z-score and changes in depressive symptoms. Individual z-scores are derived from mean timeseries extracted from significant clusters. (b) Association between changes in anxious symptoms (D RCADS) and changes in functional connectivity (D z-score). Changes are calculated as score after three months minus score on baseline. Dots represent individual associations between changes in z-score and changes in anxious symptoms. Individual z-scores are derived from mean timeseries extracted from significant clusters. CDI: Children's Depression Inventory. RCADS: Revised Child Anxiety and Depression Scale.

Discussion

In this study, we investigated longitudinal development of FC in a cohort of adolescents with internalizing disorders (e.g. with clinical depression and at least one comorbid anxiety disorder) who started care-as-usual and their healthy peers over the course of three months. Specifically, FC of amygdala subregions, the whole amygdala, and large resting-state networks derived from data-driven analysis was examined. Initial evidence was found for different FC development of the left and right laterobasal amygdala (LBA) in adolescents with internalizing disorders compared to healthy peers. Moreover, change in FC of the right LBA was associated with the overall effect of changes in anxious and depressive symptoms in INT.

To start, development of FC between the left LBA and frontal pole was significantly different between patients and healthy peers (Figure 1C). Further analyses revealed that over time, FC increased in patients but did not change in healthy peers (Figure 1E). There were no significant associations between changes in FC of the left LBA and changes in anxiety symptoms (measured with the RCADS), depressive symptoms (measured with the CDI) or an overall effect of these symptom changes in the INT group. This difference in FC development of the left LBA to the frontal pole between INT and HC fits nicely with current models of corticolimbic network dysregulation in affective disorders, in which abnormal processing within and between regions involved in cognitive control (i.e. prefrontal cortices) and emotions (i.e. limbic structures) are thought to be part of neurobiological mechanisms underlying depression and anxiety disorders [3, 4]. The frontal pole, a distinct segment within the frontal cortex, maintains both functional and structural connections with the LBA, thereby positing its likely involvement in the regulation of affective and social-cognitive abilities [84]. Indeed, changes in function and structure of the LBA and the frontal pole have frequently been reported in cross-

sectional studies on adolescent and adult internalizing disorders and thus support models concerning corticolimbic dysregulation [2, 85, 86]. This finding is also generally in line with previous longitudinal studies, which have reported increases in FC between the entire amygdala and frontal regions over time in depressed adolescents. For example, three studies demonstrated an increase in FC of the amygdala to the bilateral prefrontal cortex (PFC) [24], left medial PFC [25] and the dorsal anterior cingulate cortex [26] after several weeks of psychotherapy (either five weeks or at least six sessions of CBT or 16 weeks of interpersonal psychotherapy, resp.). Interestingly, in two studies, some of these findings correlated with improvement of depression severity [24, 26], but this result was not replicated in the study by Villa et al. [25] nor in the present study. Another study in depressed adolescents reported an increase in amygdala FC to the right medial and middle frontal gyri after eight weeks of selective serotonin reuptake inhibitor (SSRI) treatment [27], which was again associated with a decrease of depressive symptoms. Considering these results, we cautiously propose that the increase in FC to the frontal pole in patients could be due to a nonspecific effect of treatment, regardless of which treatment is offered. However, the control group were healthy adolescents rather than a non-treated patient group, due to ethical concerns of withholding treatment. Therefore, we cannot conclude whether this increase was due to treatment effects or non-specific effects of improvement in symptoms related to time. Nonetheless, our hypothesis is supported by the fact that previous studies showed a similar pattern of increased FC between the amygdala and frontal regions related to treatment, while all investigated different treatment methods. The lower functional coupling to regulatory regions in the frontal cortex, such as the frontal pole, at baseline could reflect aberrant psychophysiology, while the increase in FC to the frontal pole over time possibly mirrors new skills learned in treatment, although we did not find an association between this FC change and symptom levels as measured with the RCADS and CDI. We cautiously hypothesize that the changes in FC might reflect adaptive changes or nonspecific effects of treatments. Furthermore, internalizing disorders have a wide range of symptoms, which are only partly captured by questionnaires like the RCADS and CDI. Perhaps other symptoms, which are not measured by these questionnaires, would be associated with these FC changes.

Second, using the right LBA as a seed region, a significant group x time interaction between groups was found in FC to the right postcentral gyrus (Figure 1D). Further analyses revealed no effect of time within each group (Figure 1F). However, changes in connectivity to the postcentral gyrus were associated with the overall effect of changes in anxious and depressive symptoms within INT. Other associations with only anxious or depressive symptoms were not significant. Structural and functional studies have confirmed connectivity between the amygdala and sensorimotor regions, including the postcentral gyrus [87]. Functionally, the amygdala-sensorimotor pathway is involved in multiple steps of emotion processing, among others emotion recognition and emotional regulation [9, 88, 89]. For example, high levels of activation in this pathway have been reported when attention is focused on emotional state and in response to unconscious perceived threats [88]. Previous findings concerning this pathway in internalizing disorders are inconsistent and the relation to clinical symptoms in adolescents is unknown. However, one study demonstrated increased FC of the amygdala as a whole to the postcentral gyrus in adolescents with depression [90] and increased grey matter volume of the postcentral gyrus has been

reported in adolescents with anxious depression, but not in healthy controls or depressed adolescents [91]. Because the overall effect of symptom changes was associated with FC change in the right LBA-postcentral gyrus pathway, we posit that the amygdala-sensorimotor pathway might be especially involved in internalizing psychopathology with anxiety *and* depressive components, although the specific role of the LBA remains to be investigated.

Taken together, these results indicate that FC development of amygdala subregions is different in adolescents with internalizing disorders while they receive case-as-usual compared to healthy peers. Results were specifically located in FC of the LBA, a subregion connected to, among others, frontal regions, while analyses on FC of the CMA, mainly connected to the brainstem nuclei that generate behavioral and visceral correlates of acute stress-reactions [11-13], and analyses on FC of the whole amygdala did not reveal any significant interactions. Therefore, these results provide more insight in involvement of amygdala subregions in adolescent internalizing disorders and highlight the importance of differentiation between these subregions.

These findings are generally in line with previous work on longitudinal data of the EPISCA study, where we have demonstrated greater baseline cross-sectional connectivity of the uncinate fasciculus (UF), a white matter tract connecting the amygdala to the frontal cortex [37] and greater full amygdala FC to the dorsolateral prefrontal cortex (dlPFC) in adolescents with internalizing disorders compared to healthy peers [35], although longitudinal analyses on white matter revealed no changes in the UF [34].

Interestingly, we did not find any changes in FC of large resting-state networks derived from ICA. This could be due to several reasons, such as our sample size, which might be too small relative to the complexity of our data, or the time frame, which might not be long enough to detect any differences between groups over time. Our findings are in line with a large recent population-based study in adolescents with internalizing symptoms, which reported small changes in FC from ICA derived networks over four years that did not survive multiple testing correction [92].

Strengths, limitations & future research

This study is unique in the way that it investigated FC of amygdala subregions and data-driven whole-brain networks in a heterogeneous cohort of adolescents with internalizing psychopathology. This approach offers possibilities to expand our knowledge of FC development in adolescents with internalizing disorders compared to the healthy population, while simultaneously reflecting the clinical practice in which adolescents typically receive personalized treatment, focused on their individual needs. However, a few limitations of the present study need to be mentioned. First, this study design did not use a standardized treatment protocol but followed patients over three months' time, while they received care-as-usual; thus, it does not allow to evaluate treatment efficacy and any precise hypotheses about underlying specific reasons *why* FC and disease severity change in this population are relatively hard to generate. However, this study design provides valuable information about *how* FC and symptoms change over time, regardless of specific interventions, and is representative of clinical practice. Second, the study

groups predominantly consisted of female participants, but the sex distribution was not significantly different between the clinical and healthy control group. Yet, as girls are more likely to develop internalizing psychopathology and the female sex has been associated with an increased risk of comorbid anxiety and depression, we feel our study is representative of the clinical population although the sex ratio might be more unbalanced compared to ratios reported in current literature [93, 94]. Third, due to the imbalance in sex within groups, correction for sex was not possible, even though a mediating role in FC development has been reported [95]. Fourth, sample size and study duration were modest. In this heterogeneous group, adolescents were diagnosed with at least one out of five anxiety disorders as noted in Table 1 while receiving variants of personalized treatment as noted in Supplemental Table S1, and the sample reflected the adolescence in ages ranging from 12 to 20. In the light of the small sample size, this heterogeneous group could make interpretation of results difficult. With regards to the study duration, previous longitudinal studies in adolescents with internalizing disorders have assessed longitudinal effects of cognitive behavioral therapy (CBT) over three months and reported functional brain changes in amygdalar – prefrontal connections, which in some studies were associated with improvement of clinical symptoms [25, 96-98]. Taken together, we feel our sample represents clinical practice as close as possible and is thus indicative of the development of neural networks across adolescence in the real world, and we expected three months to be sufficient to detect any changes. Fifth, interpretation of results is limited as we did not include a clinical control group due to ethical reasons. Sixth, results did not stand after FDR correction for multiple testing across seeds and hemispheres. Lastly, information about social-economic status or illness duration was not collected and therefore could not be accounted for.

Future research could focus on several aspects. First, previous studies used different interventions and timespans, complicating comparison and generalization of the results. Therefore, a project within a large consortium like the ENIGMA-Anxiety Working Group might be interesting to pool imaging data, increase sample size and improve reliability of results within a mega- or meta-analysis [16, 28, 99]. Second, future studies should consider longitudinal investigation of amygdala subregions to further explore their unique role in adolescent internalizing disorders. Third, this study provides new insights in amygdala FC development in this population, which could lead to identifying possible new targets for innovative treatments such as fMRI-based neurofeedback [100-102]. Fourth, future studies could consider more frequent assessment in a large timeframe to detect small FC changes in ICA derived networks.

Conclusion

Concluding, this study provides initial evidence that FC development over the course of three months is different in adolescents with internalizing disorders who receive care-as-usual compared to their healthy peers, possibly reflecting nonspecific treatment effects, and highlights the importance of differentiation of amygdala subregions.

Supplemental methods

Participants

The first group, adolescents with internalizing disorders (INT), were included in the study before start of care-as-usual and recruited in outpatient departments of two child-and-adolescent psychiatric clinics. They were (i) diagnosed with clinical depression and at least one clinical anxiety disorder as assessed by categorical measures of DSM-IV depressive or anxiety disorders, (ii) were being referred for cognitive behavioral therapy at an out-patient care unit, and (iii) had no current or prior use of antidepressants except for stable SSRI use during the course of the study (n = 2).

The second group consisted of healthy control peers (HC), who were recruited through local advertisements. They had (i) no current or past DSM-IV diagnoses of Axis I and/or Axis II disorders, (ii) no clinical scores on validated mood and behavioral questionnaires, (iii) no history of traumatic experiences, and (iv) no current psychotherapeutic and/or psychopharmacological intervention of any kind.

Exclusion criteria for both groups were: (i) a primary DSM-IV diagnosis of attention deficit hyperactivity disorder, oppositional defiant disorder, conduct disorder, pervasive developmental disorders, posttraumatic stress disorder, Tourette's syndrome, obsessive–compulsive disorder, bipolar disorder, and psychotic disorders, (ii) current use of psychotropic medication, (iii) current substance abuse, (iv) a history of neurological disorders or severe head injury, (v) age < 12 or > 21 years, (vi) pregnancy, (vii) left-handedness, (viii) IQ score < 80, as measured by either the Wechsler Intelligence Scale for Children (WISC; Wechsler [103]) or the Wechsler Adult Intelligence Scale (WAIS; Wechsler [104]), and (ix) general MRI contraindications (e.g. metal implants, claustrophobia).

At the first visit, participants underwent clinical assessment by a child and adolescent psychiatrist. Afterwards, the Anxiety Disorders Interview Schedule (ADIS; Silverman *et al.* [105]) was performed to obtain DSM-IV-based classifications of anxiety and depressive disorders. To assess severity of anxious and depressive symptoms, additional self-report questionnaires were completed at each visit, including the Children's Depression Inventory (CDI; Kovacs [57]) and the Revised Child Anxiety and Depression Scale (RCADS; Chorpita *et al.* [58]). Pubertal stage was assessed using the self-report Pubertal Development Scale (PDS; Petersen *et al.* [59]), according to the following categories: 1) prepubertal, 2) early pubertal, 3) midpubertal, 4) late pubertal, and 5) postpubertal. HC-participants were excluded when criteria for a (history of) DSM-IV diagnosis or (sub)clinical scores on clinical questionnaires were met.

Ethics

The EPISCA study was approved by the medical ethics committee of Leiden University Medical Center. All participants provided informed consent according to the Declaration of Helsinki; both participants and parents signed the informed consent form. All anatomical scans were reviewed by a radiologist.

Analysis of demographic data and symptom severity

To examine differences in demographic data between the two groups, and within-subject changes of symptoms in the INT group, (paired) t-tests or two-sided Fisher exact tests were used for continuous and dichotomous data respectively. For non-normally distributed data, as defined by a significant Shapiro-Wilk test, the Mann-Whitney U test or Wilcoxon signed-rank test were used. A limited number of items were missing in the CDI questionnaire (10 items in total, 6 items for 6 participants at session 1 and 4 items for 1 participant at session 2) and in the RCADS (4 items in total, 3 items for 3 participants at session 1 and 1 item for 1 participant at session 2). Expectation maximization was allowed as Little's MCAR tests showed that data was completely missing at random for both questionnaires at both sessions.

The Bonferroni method was used to correct p-values for multiple comparisons (4 tests, being comparisons on each timepoint of scores on the RCADS and CDI between the INT and HC group, corrected p-value = 0.0125).

MRI data acquisition

Data were collected using a Philips 3.0 T Achieva MRI scanner (Philips Medical Systems, The Netherlands) with an eight-channel sensitivity encoding (SENSE) head coil. Resting-state functional MRI data were acquired for each subject using T2*-weighted gradient echo-planar imaging (EPI) with the following scan parameters: 160 whole-brain volumes; repetition time (TR) 2200 ms; echo time (TE) 30 ms; flip angle 80°; 38 transverse slices; no slice gap; field of view 220 mm; in-plane voxel size 2.75 x 2.75 mm; slice thickness 2.72 mm; total duration of the resting-state run 6 minutes.

Participants were instructed to lie still with their eyes closed and not to fall asleep. Wakefulness during acquisition was confirmed after the scan. In addition, a sagittal 3-dimensional gradient-echo T1-weighted image was acquired for registration purposes with the following scan parameters: TR 9.8 ms; TE 4.6 ms; flip angle=8°; 192 x 152 matrix; FOV 224 x 177 x 168 mm, 140 sagittal slices; no slice gap; 1.16 x 1.16 x 1.20 mm voxels. Lastly, a high-resolution EPI scan was acquired for registration purposes with the following scan parameters: TR 2200 ms; TE 30 ms; flip angle = 80°; 112 x 109 matrix; FOV 220 x 220 x 168 mm, 84 sagittal slices; no slice gap; 1.96 x 1.96 x 2 mm voxels. Prior to scanning, all participants were introduced to the scanning situation by lying in a dummy scanner and hearing scanner sounds.

Supplemental results

Table S1 Overview of treatments received by participants.

Combination of treatments	Number of participants (n)
CBT	8
CBT + family therapy	12
CBT + EMDR	1
Creative therapy + family therapy	1
None started	1

CBT: cognitive behavioral therapy. EMDR: Eye Movement Desensitization and Reprocessing. Creative therapy was received in a group setting.

Table S2 Peak coordinates of intrinsic functional connectivity using amygdala subregions (SCA).

Seed	Clusters	Cluster size	z-score	X	Y	Z	Regions in cluster
Left CMA	1	31372	15.4	-26	-6	-26	Thalamus, putamen, pallidum, hippocampus, amygdala, accumbens, temporal pole (bilateral)
	2	12144	7.32	4	20	42	Paracingulate gyrus, ACC, superior frontal gyrus
	3	5409	6.39	36	56	22	Frontal pole (right)
	4	3883	6.36	-36	46	26	Frontal pole (left)
Right CMA	1	26793	14.3	26	-4	-26	Amygdala, hippocampus, temporal pole, parahippocampal gyrus (bilateral)
	2	584	4.74	-24	32	-8	Frontal orbital cortex, frontal pole (right)
	3	7309	6.22	-8	-64	66	Lateral occipital cortex, precuneous cortex (left)
	4	2558	6.49	40	52	28	Frontal pole (right)
	5	2311	5.58	-38	52	14	Frontal pole (left)
Left LBA	1	13435	15.6	-22	-10	-10	Amygdala, hippocampus, putamen, superior temporal gyrus (bilateral)
	2	4547	4.94	-8	-76	46	Precuneous cortex, lateral occipital cortex (bilateral)
	3	820	4.65	4	-38	38	Posterior cingulate cortex, postcentral gyrus, precentral gyrus (bilateral)
Right LBA	1	11294	15.9	26	-10	-8	Amygdala, pallidum, putamen, hippocampus (bilateral)
	2	1897	4.56	-48	-52	56	Supramarginal gyrus, angular gyrus (left)
	3	1411	4.74	14	-72	48	Precuneal cortex, lateral occipital cortex (right)

CMA: centromedial amygdala. LBA: laterobasal amygdala.

Table S3 Peak coordinates of ICA derived networks.

Network	Function	Clusters	Cluster size	z-score	X	Y	Z	Regions within cluster
Default mode	Ruminative, negative self-referential processes [106]	1	5637	9.15	-2	66	-4	Frontal pole
		2	4597	15	0	-54	30	PCC, precuneal cortex
		3	1991	10.6	-44	-66	30	Lateral occipital cortex (superior division), angular cortex (right)
		4	1052	7.39	54	-62	28	Lateral occipital cortex (superior division), angular cortex (left)
		5	1038	6.82	-66	-14	-16	Postcentral gyrus
Affective	Emotion processing and regulation [107].	1	2882	5.57	-10	8	-12	Accumbens (bilateral), thalamus, amygdala
		2	826	4.66	26	-36	-4	Hippocampus (bilateral)
Executive control	Emotion regulation and goal-directed response initiation [17]	1	22723	16.8	0	40	24	Paracingulate gyrus, ACC, frontal pole
		2	361	5.02	44	-54	-44	Cerebellum (right)
		3	259	5.9	-40	-56	-42	Cerebellum (left)
Dorsal Attention	Goal directed and visuospatial attention [108]	1	14797	11.3	22	-70	48	Lateral occipital cortex (superior division), precuneus (bilateral)
		2	1322	11	28	-6	56	Superior & middle frontal gyrus, precentral gyrus (right)
		3	722	6.16	-24	-10	54	Precentral gyrus, superior & middle frontal gyrus (left)
Frontparietal right	Attention processing [109]	1	9141	10.6	28	26	52	Middle frontal gyrus, superior frontal gyrus
		2	4258	15.5	46	-56	44	Angular gyrus, lateral occipital cortex
		3	2451	9.54	-38	-66	-42	Cerebellum
		4	2122	7.45	66	-28	-6	Middle tempral gyrus, posterior division
Frontoparietal left	Attention processing [109]	1	11542	10.6	-26	14	56	Superior frontal gyrus, middle frontal gyrus
		2	5169	13.4	-46	-52	46	Angular gyrus, supramarginal gyrus
		3	2776	10.3	30	-66	-32	Cerebellum
		4	2098	8.79	-56	-42	-14	Inferior temporal gyrus

Table S3 (continued)

Salience	External stimulus detection and processing of emotionally salient information [110]	1	8465	12.3	58	-28	22	Insula, putamen, thalamus, parietal operculum cortex, supramarginal gyrus (right)
		2	7561	11.4	-56	-28	16	Insula, putamen, thalamus, parietal operculum cortex, supramarginal gyrus (left)
		3	1737	7.63	6	-2	48	ACC, juxtapositional lobule cortex (bilateral)
		4	111	4.95	-22	-46	60	Superior parietal lobule, postcentral gyrus (right)

Table S4 Design modeling multilevel block permutations to investigate voxelwise group x time interactions and effects of time within groups.

Table S5 Design modeling multilevel block permutations to investigate voxelwise associations between FC changes and symptom changes within INT group.

Due to their size, these tables are available using the QR code below.

Table S6 Effects of time on FC of significant seeds within groups.

	Cluster	Voxels	p-value	MNI coordinates			Regions involved
				X	*Y*	*Z*	
Left LBA seed							
Positive effect of time within INT group [a]	1	347	0.009	-6	64	-10	Frontal Pole, Paracingulate Gyrus, Medial Frontal Cortex
Negative effect of time within INT group [a]	1	1288	0.002	48	-42	60	Supramarginal Gyrus, Postcentral Gyrus, Angular Gyrus, Superior Parietal Lobule
	2	6	0.048	32	-54	66	Superior Parietal Lobule
Effect of time within HC group [a]	Æ	Æ	Æ	Æ	Æ	Æ	
Right LBA seed							
Effect of time within INT group [a]	Æ	Æ	Æ	Æ	Æ	Æ	
Effect of time within HC group [a]	Æ	Æ	Æ	Æ	Æ	Æ	
Association with symptom change [b]	1	30	0.032	-56	-4	34	Precentral Gyrus, Postcentral Gyrus
	2	13	0.037	66	-8	10	Postcentral Gyrus, Central Opercular Cortex, Precentral Gyrus
	3	3	0.049	54	-14	30	Postcentral Gyrus

LBA: laterobasal amygdala. INT: internalizing group. HC: healthy control group. Æ: no significant difference. [a] Positive and negative effects of time within groups are investigated using design 1 provided in Supplemental Spreadsheet 1. [b] Associations with symptom changes are investigated using design 2 provided in Supplemental Spreadsheet 2. Threshold-free cluster enhancement (TFCE) and family-wise error (FWE) corrected at p-values < 0.05

Table S7 Coordinates of significant clusters in group x time interaction in sensitivity analyses including age as covariate.

	Cluster	Voxels	p-value	MNI coordinates			Regions involved
				X	*Y*	*Z*	
Left LBA seed without age covariate	1	581	0.003	0	50	-6	Frontal Pole; Frontal Medial Cortex; Paracingulate Gyrus; Anterior Cingulate Gyrus
Left LBA seed with age covariate	4	50	0.038	0	50	-6	Frontal Medial Cortex; Paracingulate Gyrus
	3	19	0.044	-8	60	2	Frontal Pole
	2	12	0.047	4	34	-6	Anterior Cingulate Gyrus
	1	1	0.05	6	28	-8	Subcallosal Cortex

LBA: laterobasal amygdala. Threshold-free cluster enhancement (TFCE) and family-wise error (FWE) corrected at p-values < 0.05.

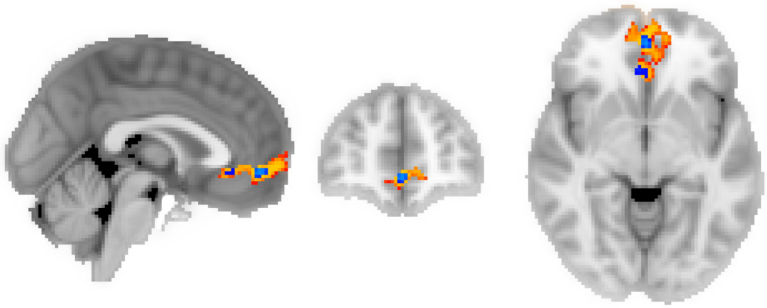

Figure S1 Different development of left LBA FC in adolescents with internalizing disorders compared to healthy peers in sensitivity analyses including age as covariate. Significant group x time interaction in left LBA FC to the frontal pole (INT (T2 > T1) > HC (T2 > T1)), coordinates of displayed slices (MNI, x, y, z): 0, 50, -6. Red represents results without age as covariate, blue represents results including age as covariate.

References

1. Melton, T.H., et al., *Comorbid Anxiety and Depressive Symptoms in Children and Adolescents: A Systematic Review and Analysis.* J Psychiatr Pract, 2016. **22**(2): p. 84-98.
2. Toenders, Y.J., et al., *Neuroimaging predictors of onset and course of depression in childhood and adolescence: A systematic review of longitudinal studies.* Dev Cogn Neurosci, 2019. **39**: p. 100700.
3. Swartz, J.R. and C.S. Monk, *The role of corticolimbic circuitry in the development of anxiety disorders in children and adolescents.* Curr Top Behav Neurosci, 2014. **16**: p. 133-48.
4. Bas-Hoogendam, J.M., et al., *Pathogenesis of social anxiety disorder*, in *The American Psychiatric Association Publishing Textbook of Anxiety, Trauma, and OCD-Related Disorders, Third Edition*, N. Simon, et al., Editors. 2020, American Psychiatric Association Publishing: Washington, DC.
5. Buckner, R.L., et al., *The organization of the human cerebellum estimated by intrinsic functional connectivity.* J Neurophysiol, 2011. **106**(5): p. 2322-45.
6. Yeo, B.T., et al., *The organization of the human cerebral cortex estimated by intrinsic functional connectivity.* J Neurophysiol, 2011. **106**(3): p. 1125-65.
7. Cole, D.M., S.M. Smith, and C.F. Beckmann, *Advances and pitfalls in the analysis and interpretation of resting-state FMRI data.* Front Syst Neurosci, 2010. **4**: p. 8.
8. Lee, M.H., C.D. Smyser, and J.S. Shimony, *Resting-state fMRI: a review of methods and clinical applications.* AJNR Am J Neuroradiol, 2013. **34**(10): p. 1866-72.
9. Tomasi, D. and N.D. Volkow, *Association between functional connectivity hubs and brain networks.* Cereb Cortex, 2011. **21**(9): p. 2003-13.
10. Beckmann, C.F., *Modelling with independent components.* Neuroimage, 2012. **62**(2): p. 891-901.
11. Duvarci, S. and D. Pare, *Amygdala microcircuits controlling learned fear.* Neuron, 2014. **82**(5): p. 966-80.
12. Janak, P.H. and K.M. Tye, *From circuits to behaviour in the amygdala.* Nature, 2015. **517**(7534): p. 284-92.
13. LeDoux, J., *The amygdala.* Curr Biol, 2007. **17**(20): p. R868-74.
14. Michely, J., et al., *Distinct Processing of Aversive Experience in Amygdala Subregions.* Biol Psychiatry Cogn Neurosci Neuroimaging, 2020. **5**(3): p. 291-300.
15. Tang, S., et al., *Abnormal amygdala resting-state functional connectivity in adults and adolescents with major depressive disorder: A comparative meta-analysis.* EBioMedicine, 2018. **36**: p. 436-445.
16. Zugman, A., et al., *A systematic review and meta-analysis of resting-state fMRI in anxiety disorders: Need for data sharing to move the field forward.* J Anxiety Disord, 2023. **99**: p. 102773.
17. Miller, E.K. and J.D. Cohen, *An integrative theory of prefrontal cortex function.* Annu Rev Neurosci, 2001. **24**: p. 167-202.
18. Tse, N.Y., et al., *Functional dysconnectivity in youth depression: Systematic review, meta-analysis, and network-based integration.* Neurosci Biobehav Rev, 2023. **153**: p. 105394.
19. Casey, B.J., R.M. Jones, and T.A. Hare, *The adolescent brain.* Ann N Y Acad Sci, 2008. **1124**: p. 111-26.
20. Crone, E.A., *Executive functions in adolescence: inferences from brain and behavior.* Dev Sci, 2009. **12**(6): p. 825-30.
21. Vink, M., et al., *Functional differences in emotion processing during adolescence and early adulthood.* Neuroimage, 2014. **91**: p. 70-6.
22. Baumel, W.T., et al., *Neurocircuitry of treatment in anxiety disorders.* Biomark Neuropsychiatry, 2022. **6**.
23. Chattopadhyay, S., et al., *Cognitive Behavioral Therapy Lowers Elevated Functional Connectivity in Depressed Adolescents.* EBioMedicine, 2017. **17**: p. 216-222.
24. Straub, J., et al., *Successful group psychotherapy of depression in adolescents alters fronto-limbic resting-state connectivity.* J Affect Disord, 2017. **209**: p. 135-139.
25. Villa, L.M., et al., *Cognitive behavioral therapy may have a rehabilitative, not normalizing, effect on functional connectivity in adolescent depression.* J Affect Disord, 2020. **268**: p. 1-11.
26. Klimes-Dougan, B., et al., *Structural and Functional Neural Correlates of Treatment Response for Interpersonal Psychotherapy for Depressed Adolescents.* J Clin Med, 2022. **11**(7).
27. Cullen, K.R., et al., *Neural Correlates of Antidepressant Treatment Response in Adolescents with Major Depressive Disorder.* J Child Adolesc Psychopharmacol, 2016. **26**(8): p. 705-712.
28. Bas-Hoogendam, J.M., et al., *ENIGMA-anxiety working group: Rationale for and organization of large-scale neuroimaging studies of anxiety disorders.* Hum Brain Mapp, 2022. **43**(1): p. 83-112.
29. Xu, J., et al., *Anxious brain networks: A coordinate-based activation likelihood estimation meta-analysis of resting-state functional connectivity studies in anxiety.* Neurosci Biobehav Rev, 2019. **96**: p. 21-30.
30. Singh, S.P., et al., *Mind the gap: the interface between child and adult mental health services.* Psychiatric Bulletin, 2018. **29**(8): p. 292-294.
31. Walter, H.J., et al., *Clinical Practice Guideline for the Assessment and Treatment of Children and Adolescents With Anxiety Disorders.* J Am Acad Child Adolesc Psychiatry,

2020. **59**(10): p. 1107-1124.

32. Walter, H.J., et al., *Clinical Practice Guideline for the Assessment and Treatment of Children and Adolescents With Major and Persistent Depressive Disorders.* J Am Acad Child Adolesc Psychiatry, 2023. **62**(5): p. 479-502.
33. van den Bulk, B.G., et al., *How stable is activation in the amygdala and prefrontal cortex in adolescence? A study of emotional face processing across three measurements.* Dev Cogn Neurosci, 2013. **4**: p. 65-76.
34. Roelofs, E.F., et al., *Exploring the course of adolescent anxiety and depression: associations with white matter tract microstructure.* Eur Arch Psychiatry Clin Neurosci, 2022. **272**(5): p. 849-858.
35. Pannekoek, J.N., et al., *Aberrant resting-state functional connectivity in limbic and salience networks in treatment--naive clinically depressed adolescents.* J Child Psychol Psychiatry, 2014. **55**(12): p. 1317-27.
36. Pannekoek, J.N., et al., *Reduced anterior cingulate gray matter volume in treatment-naive clinically depressed adolescents.* Neuroimage Clin, 2014. **4**: p. 336-42.
37. Aghajani, M., et al., *Altered white-matter architecture in treatment-naive adolescents with clinical depression.* Psychol Med, 2014. **44**(11): p. 2287-98.
38. van den Bulk, B.G., et al., *Amygdala habituation to emotional faces in adolescents with internalizing disorders, adolescents with childhood sexual abuse related PTSD and healthy adolescents.* Dev Cogn Neurosci, 2016. **21**: p. 15-25.
39. van Hoof, M.J., et al., *Emotional face processing in adolescents with childhood sexual abuse-related posttraumatic stress disorder, internalizing disorders and healthy controls.* Psychiatry Res Neuroimaging, 2017. **264**: p. 52-59.
40. van den Bulk, B.G., et al., *Amygdala activation during emotional face processing in adolescents with affective disorders: the role of underlying depression and anxiety symptoms.* Front Hum Neurosci, 2014. **8**: p. 393.
41. van Hoof, M.J., et al., *Unresolved-disorganized attachment adjusted for a general psychopathology factor associated with atypical amygdala resting-state functional connectivity.* Eur J Psychotraumatol, 2019. **10**(1): p. 1583525.
42. Riem, M.M.E., et al., *General psychopathology factor and unresolved-disorganized attachment uniquely correlated to white matter integrity using diffusion tensor imaging.* Behav Brain Res, 2019. **359**: p. 1-8.
43. Rinne-Albers, M.A., et al., *Abnormalities of white matter integrity in the corpus callosum of adolescents with PTSD after childhood sexual abuse: a DTI study.* Eur Child Adolesc Psychiatry, 2016. **25**(8): p. 869-78.
44. Aghajani, M., et al., *Abnormal functional architecture of amygdala-centered networks in adolescent posttraumatic stress disorder.* Hum Brain Mapp, 2016. **37**(3): p. 1120-35.
45. van Hoof, M.J., et al., *Adult Attachment Interview differentiates adolescents with Childhood Sexual Abuse from those with clinical depression and non-clinical controls.* Attach Hum Dev, 2015. **17**(4): p. 354-75.
46. Rinne-Albers, M.A., et al., *Preserved cortical thickness, surface area and volume in adolescents with PTSD after childhood sexual abuse.* Sci Rep, 2020. **10**(1): p. 3266.
47. Rinne-Albers, M.A., et al., *Anterior cingulate cortex grey matter volume abnormalities in adolescents with PTSD after childhood sexual abuse.* Eur Neuropsychopharmacol, 2017. **27**(11): p. 1163-1171.
48. van Velzen, L.S., et al., *White matter disturbances in major depressive disorder: a coordinated analysis across 20 international cohorts in the ENIGMA MDD working group.* Mol Psychiatry, 2020. **25**(7): p. 1511-1525.
49. de Kovel, C.G.F., et al., *No Alterations of Brain Structural Asymmetry in Major Depressive Disorder: An ENIGMA Consortium Analysis.* Am J Psychiatry, 2019. **176**(12): p. 1039-1049.
50. Wang, X., et al., *Cortical volume abnormalities in posttraumatic stress disorder: an ENIGMA-psychiatric genomics consortium PTSD workgroup mega-analysis.* Mol Psychiatry, 2021. **26**(8): p. 4331-4343.
51. Dennis, E.L., et al., *Altered white matter microstructural organization in posttraumatic stress disorder across 3047 adults: results from the PGC-ENIGMA PTSD consortium.* Mol Psychiatry, 2019.
52. Han, L.K.M., et al., *Brain aging in major depressive disorder: results from the ENIGMA major depressive disorder working group.* Mol Psychiatry, 2021. **26**(9): p. 5124-5139.
53. Zhu, X., et al., *Neuroimaging-based classification of PTSD using data-driven computational approaches: A multisite big data study from the ENIGMA-PGC PTSD consortium.* Neuroimage, 2023. **283**: p. 120412.
54. van Velzen, L.S., et al., *Structural brain alterations associated with suicidal thoughts and behaviors in young people: results from 21 international studies from the ENIGMA Suicidal Thoughts and Behaviours consortium.* Mol Psychiatry, 2022. **27**(11): p. 4550-4560.
55. Sun, D., et al., *A comparison of methods to harmonize cortical thickness measurements across scanners and sites.* Neuroimage, 2022. **261**: p. 119509.
56. Sun, D., et al., *Remodeling of the Cortical Structural Connectome in Posttraumatic Stress Disorder: Results From the ENIGMA-PGC Posttraumatic Stress Disorder Consortium.* Biol Psychiatry Cogn Neurosci Neuroimaging, 2022. **7**(9): p. 935-948.
57. Kovacs, M., *The Children's Depression, Inventory (CDI).* Psychopharmacol Bull, 1985. **21**(4): p. 995-8.
58. Chorpita, B.F., et al., *Assessment of symptoms of DSM-IV*

anxiety and depression in children: a revised child anxiety and depression scale. Behav Res Ther, 2000. **38**(8): p. 835-55.

59. Petersen, A.C., et al., *A self-report measure of pubertal status: Reliability, validity, and initial norms.* J Youth Adolesc, 1988. **17**(2): p. 117-33.
60. Pruim, R.H.R., et al., *Evaluation of ICA-AROMA and alternative strategies for motion artifact removal in resting state fMRI.* Neuroimage, 2015. **112**: p. 278-287.
61. Pruim, R.H.R., et al., *ICA-AROMA: A robust ICA-based strategy for removing motion artifacts from fMRI data.* Neuroimage, 2015. **112**: p. 267-277.
62. Parkes, L., et al., *An evaluation of the efficacy, reliability, and sensitivity of motion correction strategies for resting-state functional MRI.* Neuroimage, 2018. **171**: p. 415-436.
63. Smith, S.M., *Fast robust automated brain extraction.* Hum Brain Mapp, 2002. **17**(3): p. 143-55.
64. Woolrich, M.W., et al., *Temporal autocorrelation in univariate linear modeling of FMRI data.* Neuroimage, 2001. **14**(6): p. 1370-86.
65. Jenkinson, M., et al., *Improved optimization for the robust and accurate linear registration and motion correction of brain images.* Neuroimage, 2002. **17**(2): p. 825-41.
66. Andersson, J.L.R., M. Jenkinson, and S. Smith, *Non-linear registration, aka Spatial normalisation*, in *FMRIB technical report TR07JA2*. 2007b, FMRIB Analysis Group of the University of Oxford: Oxford.
67. Jenkinson, M. and S. Smith, *A global optimisation method for robust affine registration of brain images.* Med Image Anal, 2001. **5**(2): p. 143-56.
68. Zhang, Y., M. Brady, and S. Smith, *Segmentation of brain MR images through a hidden Markov random field model and the expectation-maximization algorithm.* IEEE Trans Med Imaging, 2001. **20**(1): p. 45-57.
69. Power, J.D., et al., *Sources and implications of whole-brain fMRI signals in humans.* Neuroimage, 2017. **146**: p. 609-625.
70. Beckmann, C.F. and S.M. Smith, *Probabilistic independent component analysis for functional magnetic resonance imaging.* IEEE Trans Med Imaging, 2004. **23**(2): p. 137-52.
71. Nickerson, L.D., et al., *Using Dual Regression to Investigate Network Shape and Amplitude in Functional Connectivity Analyses.* Front Neurosci, 2017. **11**: p. 115.
72. Smith, S.M., et al., *Correspondence of the brain's functional architecture during activation and rest.* Proc Natl Acad Sci U S A, 2009. **106**(31): p. 13040-5.
73. Bas-Hoogendam, J.M., et al., *Intrinsic functional connectivity in families genetically enriched for social anxiety disorder - an endophenotype study.* EBioMedicine, 2021. **69**: p. 103445.
74. Barkhof, F., S. Haller, and S.A. Rombouts, *Resting-state functional MR imaging: a new window to the brain.* Radiology, 2014. **272**(1): p. 29-49.
75. Witt, S.T., et al., *What Executive Function Network is that? An Image-Based Meta-Analysis of Network Labels.* Brain Topogr, 2021. **34**(5): p. 598-607.
76. Pan, P.M., et al., *Ventral Striatum Functional Connectivity as a Predictor of Adolescent Depressive Disorder in a Longitudinal Community-Based Sample.* Am J Psychiatry, 2017. **174**(11): p. 1112-1119.
77. R Core Team *R: A Language and Environment for Statistical Computing*. 2023, R Foundation for Statistical Computing: Vienna, Austria.
78. Zhang, F., *Resting-State Functional Connectivity Abnormalities in Adolescent Depression.* EBioMedicine, 2017. **17**: p. 20-21.
79. Winkler, A.M., et al., *Permutation inference for the general linear model.* Neuroimage, 2014. **92**(100): p. 381-97.
80. Winkler, A.M., et al., *Multi-level block permutation.* Neuroimage, 2015. **123**: p. 253-68.
81. Smith, S.M. and T.E. Nichols, *Threshold-free cluster enhancement: addressing problems of smoothing, threshold dependence and localisation in cluster inference.* Neuroimage, 2009. **44**(1): p. 83-98.
82. Alberton, B.A.V., et al., *Multiple testing correction over contrasts for brain imaging.* Neuroimage, 2020. **216**: p. 116760.
83. Benjamini, Y. and Y. Hochberg, *Controlling the False Discovery Rate: A Practical and Powerful Approach to Multiple Testing.* Journal of the Royal Statistical Society Series B: Statistical Methodology, 1995. **57**(1): p. 289-300.
84. Bludau, S., et al., *Cytoarchitecture, probability maps and functions of the human frontal pole.* Neuroimage, 2014. **93 Pt 2**(Pt 2): p. 260-75.
85. Schmaal, L., et al., *Cortical abnormalities in adults and adolescents with major depression based on brain scans from 20 cohorts worldwide in the ENIGMA Major Depressive Disorder Working Group.* Mol Psychiatry, 2017. **22**(6): p. 900-909.
86. Bludau, S., et al., *Medial Prefrontal Aberrations in Major Depressive Disorder Revealed by Cytoarchitectonically Informed Voxel-Based Morphometry.* Am J Psychiatry, 2016. **173**(3): p. 291-8.
87. Rizzo, G., et al., *The Limbic and Sensorimotor Pathways of the Human Amygdala: A Structural Connectivity Study.* Neuroscience, 2018. **385**: p. 166-180.
88. Kropf, E., et al., *From anatomy to function: the role of the somatosensory cortex in emotional regulation.* Braz J Psychiatry, 2019. **41**(3): p. 261-269.

89. Roy, A.K., et al., *Functional connectivity of the human amygdala using resting state fMRI.* Neuroimage, 2009. **45**(2): p. 614-26.
90. Mao, N., et al., *Aberrant Resting-State Brain Function in Adolescent Depression.* Front Psychol, 2020. **11**: p. 1784.
91. Wehry, A.M., et al., *Neurostructural impact of co-occurring anxiety in pediatric patients with major depressive disorder: a voxel-based morphometry study.* J Affect Disord, 2015. **171**: p. 54-9.
92. Dall'Aglio, L., et al., *Exploring the longitudinal associations of functional network connectivity and psychiatric symptom changes in youth.* Neuroimage Clin, 2023. **38**: p. 103382.
93. Costello, E.J., et al., *Prevalence and development of psychiatric disorders in childhood and adolescence.* Arch Gen Psychiatry, 2003. **60**(8): p. 837-44.
94. Martel, M.M., *Sexual selection and sex differences in the prevalence of childhood externalizing and adolescent internalizing disorders.* Psychol Bull, 2013. **139**(6): p. 1221-59.
95. Alarcon, G., et al., *Developmental sex differences in resting state functional connectivity of amygdala sub-regions.* Neuroimage, 2015. **115**: p. 235-44.
96. Connolly, C.G., et al., *Resting-state functional connectivity of the amygdala and longitudinal changes in depression severity in adolescent depression.* J Affect Disord, 2017. **207**: p. 86-94.
97. Cyr, M., et al., *Altered network connectivity predicts response to cognitive-behavioral therapy in pediatric obsessive-compulsive disorder.* Neuropsychopharmacology, 2020. **45**(7): p. 1232-1240.
98. La Buissonniere-Ariza, V., et al., *Neural correlates of cognitive behavioral therapy response in youth with negative valence disorders: A systematic review of the literature.* J Affect Disord, 2021. **282**: p. 1288-1307.
99. Zugman, A., et al., *Mega-analysis methods in ENIGMA: The experience of the generalized anxiety disorder working group.* Hum Brain Mapp, 2022. **43**(1): p. 255-277.
100. Quevedo, K., et al., *Amygdala Circuitry During Neurofeedback Training and Symptoms' Change in Adolescents With Varying Depression.* Front Behav Neurosci, 2020. **14**: p. 110.
101. Zhang, J., et al., *Reducing default mode network connectivity with mindfulness-based fMRI neurofeedback: a pilot study among adolescents with affective disorder history.* Mol Psychiatry, 2023. **28**(6): p. 2540-2548.
102. Zich, C., et al., *Modulatory effects of dynamic fMRI-based neurofeedback on emotion regulation networks in adolescent females.* Neuroimage, 2020. **220**: p. 117053.
103. Wechsler, D., *Manual for the Wechsler Intelligence Scale for Children - Third Edition (WISC-III).* 1991, San Antonio, TX: The Psychological Corporation.
104. Wechsler, D., *Wechsler Adult Intelligence Scale.* 3rd ed. 1997, San Antonio, TX: Harcourt Assessment.
105. Silverman, W. and A.M. Albano, *The anxiety disorders interview schedule for DSM-IV - Child and parent versions.* 1996, San Antonio, TX: Raywind Publications.
106. Hamilton, J.P., et al., *Depressive Rumination, the Default-Mode Network, and the Dark Matter of Clinical Neuroscience.* Biol Psychiatry, 2015. **78**(4): p. 224-30.
107. Leppanen, J.M. and C.A. Nelson, *Tuning the developing brain to social signals of emotions.* Nat Rev Neurosci, 2009. **10**(1): p. 37-47.
108. Vossel, S., J.J. Geng, and G.R. Fink, *Dorsal and ventral attention systems: distinct neural circuits but collaborative roles.* Neuroscientist, 2014. **20**(2): p. 150-9.
109. Marek, S. and N.U.F. Dosenbach, *The frontoparietal network: function, electrophysiology, and importance of individual precision mapping.* Dialogues Clin Neurosci, 2018. **20**(2): p. 133-140.
110. Seeley, W.W., et al., *Dissociable intrinsic connectivity networks for salience processing and executive control.* J Neurosci, 2007. **27**(9): p. 2349-56.